Swarm Intellingence
Bridge Experiment with Overcrowding

Sébastien Cuendet & Jean-Philippe Pellet
{sebastien.cuendet, jean-philippe.pellet}@epfl.ch

February 5, 2006

1 Introduction

The bridge experiment [1, 2] is a classical configuration used to explain the trail laying/following mechanism; it also gave much of the inspiration to research on Ant Colony Optimization algorithms [3, 4]. In the course, we studied the bridge experiment with two branches of the same length. In this project, the more general case of two branches of different length is considered. We present both a microscopic model and a macroscopic model taking into account collision avoidance. We study the effect of the different parameters of the microscopic model (e.g. pheromone evaporation rate, initial number of ants, ratio of the path lengths) and try to find the optimal evaporation rate as a function of this ratio.

2 Microscopic and Macroscopic Model

2.1 Experiment Description and Assumptions

The experiment involves n homogeneous agents (ants, robots) in an initial position called Nest (N). Their goal is to maximize the food quantity brought back to the nest. The food source (F) can be reached by taking either a short path S of length l or a longer path L of length $r \cdot l$, $r \geq 1$. Either path is also possible on the way back to the nest independently from the path used to arrive at the food source. This is illustrated in Figure 1.

We further make the following assumptions:

- All robots have the same speed.
- The robots cannot get lost and must not have the possibility to get stuck in some state; i.e., the probability that any robot not in the nest eventually returns to the nest is 1.
- When they are on the long or short path, the robots perform collision avoidance with other robots.
- In general, the wall avoidance and U-turn phenomena are neglected in this experiment.
- The total probability of leaving the nest is small and initially equal for both paths.

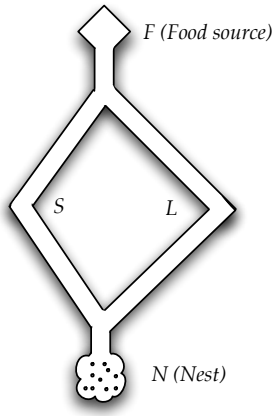

FIG. 1: Experiment schema

2.2 Microscopic Model

The microscopic model is a probabilistic final state machine (PFSM) as shown in figure Figure 2.

Apart from the nest N and the food source F, the PFSM can be divided into the states belonging to the short path on the left, and those belonging to the long path on the right. S_1 and L_1 model the paths from the nest to the source, and S_2 and L_2 the paths from the source back to the nest. The state A_X is

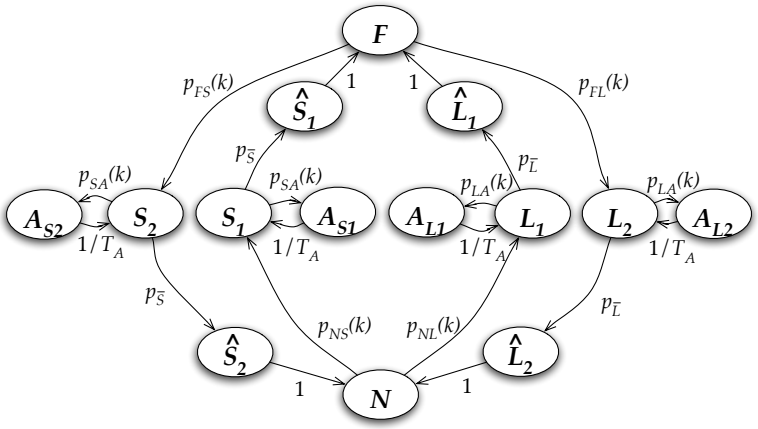

FIG. 2: The probabilistic FSM describing the microscopic model

the avoidance state corresponding to state X; the state $\widehat{X}$ is the exit state of state X and is used to model pheromones. See more on this below.

In general, p_{XY} stands for the probability per time step to make a transition from state X to state Y, and $p_{\overline{X}}$ is the probability per time step of leaving state X in direction of either the source or the nest, depending on the state.

Some of the transition probabilities are fixed; others are dynamical and written as a function of the timestep k. Their equations and the modeling decisions which were made for some aspects are detailed below.

2.2.1 Path Length

There is a ratio r between the short and the long path. The length of the path is taken into account in the probability to go from S_1 to $\widehat{S}_1$, S_2 to $\widehat{S}_2$, L_1 to $\widehat{L}_1$ and L_2 to $\widehat{L}_2$. These probabilities $p_{\overline{S}}$ and $p_{\overline{L}}$ are defined as the inverse of the time spent by a robot if it were to do through the whole path without being interrupted:

$$p_{\overline{S}} = \frac{1}{l/v} = \frac{v}{l} \qquad\qquad p_{\overline{L}} = \frac{1}{r \cdot l/v} = \frac{v}{r \cdot l} \tag{1}$$

where v is the mean speed of the robots.

This reasoning for modeling the path length also holds if the collision avoidance probabilities p_{SA} and p_{LA} change. Consider for instance that p_{SA} were to reach a value of $n \cdot p_{\overline{S}}$. A robot is then expected to exit the current state S_1 to A_{S_1} n times as often as to $\widehat{S}_1$. A full traversal of the short path is then expected to contain on average n collision avoidance maneuvers, and thus $n+1$ visits of the state S_1. The mean time T'_{S_1} spent in S_1 (computed as the inverse of the sum of all outgoing probabilities) should then be $n+1$ times shorter than if there were no collision avoidance at all (T_{S_1}). It indeed is:

$$T'_{S_1} = \frac{1}{\frac{v}{l} + n \cdot \frac{v}{l}} = \frac{1/\frac{v}{l}}{n+1} = \frac{T_{S_1}}{n+1} \tag{2}$$

2.2.2 Collision Avoidance

Collision/obstacle avoidance is only possible in state S_1, L_1, S_2 and L_2; it is neglected in all other states. The probability p_{SA} of doing obstacle avoidance is the same for S_1 and S_2 (as they model the same physical path) and depends on the number of robots in these states. The same applies to L_1 and L_2. We introduce a new model parameter, p_r, which is defined as the probability of meeting one robot on the short path. Then:

$$p_{SA}(k) = \max\left\{1 - p_{\overline{S}},\ \ p_r \cdot (S_1(k) + S_2(k) - 1)\right\} \tag{3}$$

$$p_{LA}(k) = \max\left\{1 - p_{\overline{S}},\ \ \frac{p_r}{r} \cdot (L_1(k) + L_2(k) - 1)\right\} \tag{4}$$

Obviously, an upper bound has to be defined for these probabilities in order for them not to be greater than 1 (or $1 - p_{\overline{S}}$ here). This case, however, would make sense, and corresponds to the physical situation where there are so many robots on the path that it is impossible to squeeze them more in order to have a new one enter the path. But in order to have a smooth, continuously derivable function for these probabilities in our simulation, we actually replaced Equations 3 and 4 by:

$$p_{SA}(k) = (1 - p_{\overline{S}}) \left(1 - e^{-\lambda \cdot p_r \cdot (S_1(k) + S_2(k) - 1)}\right) \tag{5}$$

$$p_{LA}(k) = (1 - p_{\overline{S}}) \left(1 - e^{-\lambda \cdot \frac{p_r}{r} \cdot (L_1(k) + L_2(k) - 1)}\right) \tag{6}$$

The factor λ is then optimized so that Equations 5 and 6 best match Equations 3 and 4, respectively. We used $\lambda = 1.5$. Also note that in Equations 4 and 6, we divide p_r by r in order to model the fact that a collision is r times less likely on a r times longer path.

The average time spent in collision avoidance, T_A, is a new model parameter. The avoidance state have been implemented probabilistically, the probability to leave any avoidance state being $1/T_A$.

2.2.3 Pheromone Trail Laying/Following

Pheromone laying is simulated by states $\widehat{S}_1$, $\widehat{L}_1$, $\widehat{S}_2$ and $\widehat{L}_2$ where the robots only spend one time step when they leave the short and the long path, respectively, in direction of the nest or the food source. This allows one to conveniently express the pheromone concentration by a sum (weighted by powers of the evaporation rate) of the number of agents in these states during the last j_{max} steps. Note that pheromones deposited while going to the food source are "smelled" when coming back from the source, and vice-versa.

$$\Phi_{NS}(k) = \sum_{j=0}^{j_{max}} h^j \cdot \widehat{S}_2(k-j) \qquad \Phi_{FS}(k) = \sum_{j=0}^{j_{max}} h^j \cdot \widehat{S}_1(k-j) \tag{7}$$

$$\Phi_{NL}(k) = \sum_{j=0}^{j_{max}} h^j \cdot \widehat{L}_2(k-j) \qquad \Phi_{FL}(k) = \sum_{j=0}^{j_{max}} h^j \cdot \widehat{L}_1(k-j) \tag{8}$$

The new model parameter h is the evaporation rate of the pheromone. The probabilities $p_{NS}(k)$, $p_{NL}(k)$, $p_{FS}(k)$, $p_{FL}(k)$ can then be modeled this way (not unlike the microscopic modeling proposed in [2]):

$$p_{NS}(k) = \frac{[q + \Phi_{NS}(k)]^n}{[q + \Phi_{NS}(k)]^n + [q + \Phi_{NL}(k)]^n} \qquad p_{FS}(k) = \frac{[q + \Phi_{FS}(k)]^n}{[q + \Phi_{FS}(k)]^n + [q + \Phi_{FL}(k)]^n} \tag{9}$$

$$p_{NL}(k) = \frac{[q + \Phi_{NL}(k)]^n}{[q + \Phi_{NS}(k)]^n + [q + \Phi_{NL}(k)]^n} \qquad p_{FL}(k) = \frac{[q + \Phi_{FL}(k)]^n}{[q + \Phi_{FS}(k)]^n + [q + \Phi_{FL}(k)]^n} \tag{10}$$

There are two new parameters: n is the degree of non-linearity and q is the degree of attraction of an unmarked branch. A higher k means more exploration, a higher n means more exploitation—they are used jointly to tune the ants' behavior towards pheromone concentration.

2.3 Macroscopic Model

Let us first review all model parameters:

r : Ration L/S	N_0 : Initial number of ants
h : Evaporation rate	$p_{\overline{N}}$: Total probability to leave the nest
q : Unmarked branch attraction	p_r : Probability to meet one robot on short branch
n : Non-linearity degree	T_A : Average avoidance time

The macroscopic model uses the same probabilities and the same states as the microscopic model presented in the previous section. The evolution of the model can be expressed by the following difference

equations (only states corresponding to the nest, the food source and the short path are described; equations for the long path can be derived similarly using Equations 12 to 17 and the symmetric properties of the paths). The initial conditions are specified as $X(0) = 0$ for all states $X \neq N$ and $N(0) = N_0$.

$$N(k+1) = N(k) + \widehat{S}_2(k) + \widehat{L}_2(k) - p_{NS} \cdot N(k) - p_{NL} \cdot N(k) \tag{11}$$
$$S_1(k+1) = S_1(k) + p_{NS} \cdot N(k) + p_{\overline{A}} \cdot A_{S_1}(k) - p_{\overline{S}} \cdot S_1(k) - p_{SA} \cdot S_1(k) \tag{12}$$
$$\widehat{S}_1(k+1) = p_{\overline{S}} \cdot S_1(k) \tag{13}$$
$$S_2(k+1) = S_2(k) + p_{FS} \cdot F(k) + p_{\overline{A}} \cdot A_{S_2}(k) - p_{\overline{S}} \cdot S_2(k) - p_{SA} \cdot S_2(k) \tag{14}$$
$$\widehat{S}_2(k+1) = p_{\overline{S}} \cdot S_2(k) \tag{15}$$
$$A_{S_1}(k+1) = A_{S_1}(k) + p_{SA} \cdot S_1(k) - p_{\overline{A}} \cdot A_{S_1}(k) \tag{16}$$
$$A_{S_2}(k+1) = A_{S_2}(k) + p_{SA} \cdot S_2(k) - p_{\overline{A}} \cdot A_{S_2}(k) \tag{17}$$
$$F(k+1) = \widehat{S}_2(k) + \widehat{L}_2(k) \tag{18}$$

3 Results

We now present some interesting results obtained by simulating the experiment in the final state machine representing the microscopic model described in the previous section. Figure 3 shows the ant proportion on the branches without pheromones with $r = 3$ and $r = 5$. They oscillate around 75%/25% and 80%/20%, respectively; this is what we expect if ants randomly choose either path. Figure 4 includes pheromone laying and shows how convergence differ depending on the initial number of ants in the nest. More ants mean naturally more influence of the better path because more pheromone is deposited. Finally, Figure 5 shows an experiment where the unmarked branch attraction q was set to 0 (down from 4) at iteration 7000. We see that the system eventually converges to a 100% exploitation of the short branch.

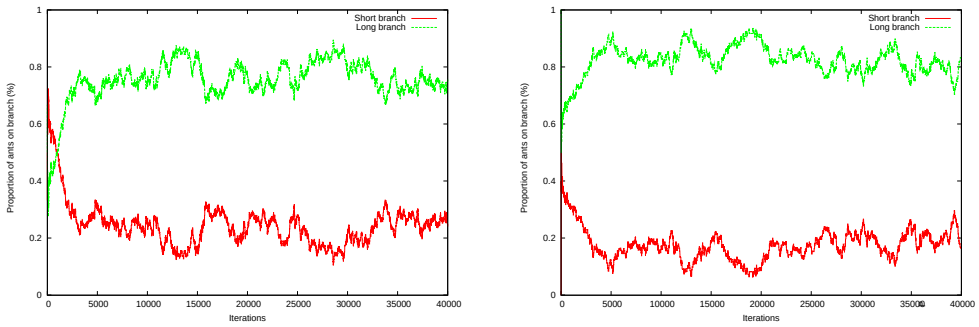

FIG. 3: Stabilization without pheromones ($h = 0$; $r = 3$ [left], $r = 5$ [right])

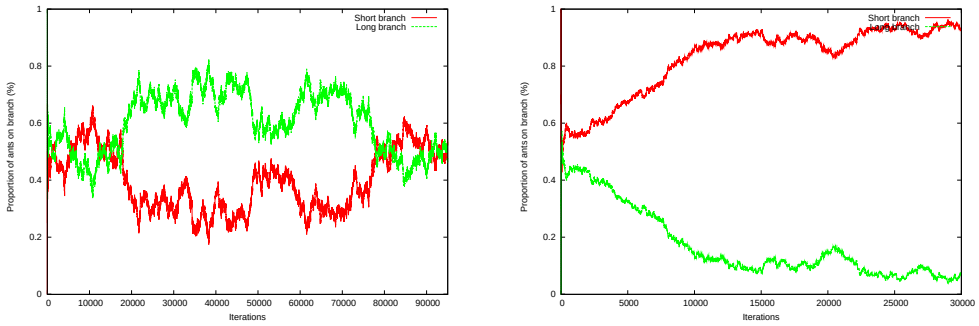

FIG. 4: Convergence with pheromones ($r = 2$; $h = 0.98$; $N_0 = 100$ [left], $N_0 = 200$ [right])

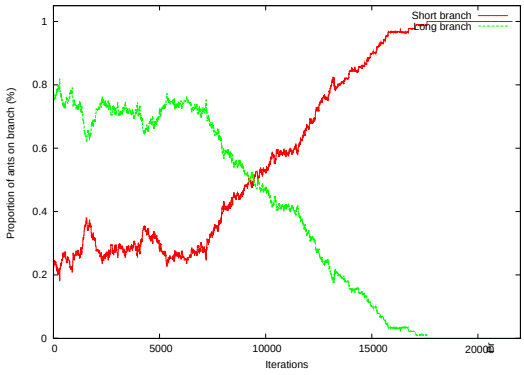

FIG. 5: Dynamic change of q at it. 7000

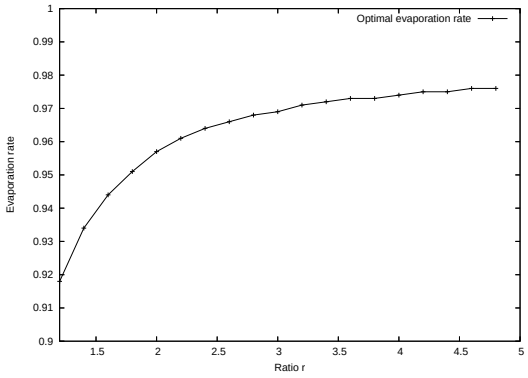

FIG. 6: Optimal h as a function of r

Optimal evaporation rate Beside n and q, the evaporation rate of the pheromone h is one of the key parameters of the experiment. If too high, the ants might get stuck in one branch and unable to go into the other one (too much *exploitation*). If too small, the ants are not able to mark enough strongly the chosen branch and continue to explore the other one even if it gives worse results (too much *exploration*). Thus, finding the optimal evaporation rate for a given context is a crucial issue. Figure 6 shows the optimal evaporation rate experimentally as a function of the ratio r between the two branches. This result was obtained by simulating the evolution of the macroscopic model for $k_{max} = 10000$ timesteps; the evaporation rates were ranked according to the following fitness function, which counts ants returning back to the nest:

$$fitness(params) = \frac{1}{N_0}\frac{1}{k_{max}}\sum_{k=1}^{k_{max}}\left[\widehat{S}_2(k) + \widehat{L}_2(k)\right] \tag{19}$$

4 Conclusion & Outlook

Including the collision avoidance mechanism in the asymmetric bridge experiments yields interesting results. The optimal pheromone evaporation should be always slower to reach a good fitness as the ratio r between the two branches increases, including the overcrowding effect. This holds of course if all assumptions are correct.

Further work on this problem would probably have to include more systematic testing and realistic simulation in order to try to reach a zero-free parameter model. Some of the parameters could be realistically approximated by making more assumptions on the size and geometry of the robots and paths, for instance. Additional problem aspects could also be taken into account, like wall avoidance, U-turn probability, noisy perception. A genetic algorithm could also be designed to optimize all free parameters to find what the optimal ant species' properties for this problem could be.

References

[1] S. Goss, S. Aron, J. L. Deneubourg and J. M. Pasteels, Self-organized shortcuts in the Argentine ant, *Naturwissenschaften*, 76:579–581, 1989.

[2] J.-L. Deneubourg, S. Aron, S. Goss and J.-M. Pasteels, The self-organizing exploratory pattern of the Argentine ant, *Journal of Insect Behavior*, 3:159–168, 1990.

[3] M. Dorigo, V. Maniezzo, and A. Colorni, *Positive feedback as a search strategy*, Technical Report 91-016, Dipartimento di Elettronica, Politecnico di Milano, Italy, 1991.

[4] M. Dorigo, *Optimization, Learning and Natural Algorithms* (in Italian), Ph.D. Thesis, Dipartimento di Elettronica, Politecnico di Milano, Italy, 1992, 140 pages.